NASA/TM-2000-209021

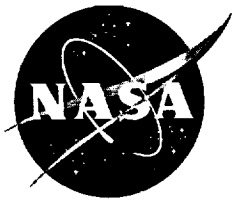

Optimal Pitch Thrust-Vector Angle and Benefits for all Flight Regimes

Glenn B. Gilyard
Dryden Flight Research Center
Edwards, California

Alexander Bolonkin
Senior Research Associate of the National Research Council
Dryden Flight Research Center
Edwards, California

March 2000

The NASA STI Program Office...in Profile

Since its founding, NASA has been dedicated to the advancement of aeronautics and space science. The NASA Scientific and Technical Information (STI) Program Office plays a key part in helping NASA maintain this important role.

The NASA STI Program Office is operated by Langley Research Center, the lead center for NASA's scientific and technical information. The NASA STI Program Office provides access to the NASA STI Database, the largest collection of aeronautical and space science STI in the world. The Program Office is also NASA's institutional mechanism for disseminating the results of its research and development activities. These results are published by NASA in the NASA STI Report Series, which includes the following report types:

- TECHNICAL PUBLICATION. Reports of completed research or a major significant phase of research that present the results of NASA programs and include extensive data or theoretical analysis. Includes compilations of significant scientific and technical data and information deemed to be of continuing reference value. NASA's counterpart of peer-reviewed formal professional papers but has less stringent limitations on manuscript length and extent of graphic presentations.

- TECHNICAL MEMORANDUM. Scientific and technical findings that are preliminary or of specialized interest, e.g., quick release reports, working papers, and bibliographies that contain minimal annotation. Does not contain extensive analysis.

- CONTRACTOR REPORT. Scientific and technical findings by NASA-sponsored contractors and grantees.

- CONFERENCE PUBLICATION. Collected papers from scientific and technical conferences, symposia, seminars, or other meetings sponsored or cosponsored by NASA.

- SPECIAL PUBLICATION. Scientific, technical, or historical information from NASA programs, projects, and mission, often concerned with subjects having substantial public interest.

- TECHNICAL TRANSLATION. English-language translations of foreign scientific and technical material pertinent to NASA's mission.

Specialized services that complement the STI Program Office's diverse offerings include creating custom thesauri, building customized databases, organizing and publishing research results...even providing videos.

For more information about the NASA STI Program Office, see the following:

- Access the NASA STI Program Home Page at ***http://www.sti.nasa.gov***

- E-mail your question via the Internet to help@sti.nasa.gov

- Fax your question to the NASA Access Help Desk at (301) 621-0134

- Telephone the NASA Access Help Desk at (301) 621-0390

- Write to:
  NASA Access Help Desk
  NASA Center for AeroSpace Information
  7121 Standard Drive
  Hanover, MD 21076-1320

NASA/TM-2000-209021

Optimal Pitch Thrust-Vector Angle and Benefits for all Flight Regimes

Glenn B. Gilyard
Dryden Flight Research Center
Edwards, California

Alexander Bolonkin
Senior Research Associate of the National Research Council
Dryden Flight Research Center
Edwards, California

National Aeronautics and
Space Administration

Dryden Flight Research Center
Edwards, California 93523-0273

March 2000

NOTICE

Use of trade names or names of manufacturers in this document does not constitute an official endorsement of such products or manufacturers, either expressed or implied, by the National Aeronautics and Space Administration.

Available from the following:

NASA Center for AeroSpace Information (CASI)
7121 Standard Drive
Hanover, MD 21076-1320
(301) 621-0390

National Technical Information Service (NTIS)
5285 Port Royal Road
Springfield, VA 22161-2171
(703) 487-4650

ABSTRACT

The NASA Dryden Flight Research Center is exploring the optimum thrust-vector angle on aircraft. Simple aerodynamic performance models for various phases of aircraft flight are developed and optimization equations and algorithms are presented in this report. Results of optimal angles of thrust vectors and associated benefits for various flight regimes of aircraft (takeoff, climb, cruise, descent, final approach, and landing) are given. Results for a typical wide-body transport aircraft are also given. The benefits accruable for this class of aircraft are small, but the technique can be applied to other conventionally configured aircraft. The lower L/D aerodynamic characteristics of fighters generally would produce larger benefits than those produced for transport aircraft.

NOMENCLATURE

a, b, c	quadratic equation coefficients
A_x	acceleration along the flightpath axis
C_D	drag coefficient
C_{D_o}	minimum C_D
C_L	lift coefficient; $W/(qS)$
C_{L_f}	lift coefficient caused by flap deflection
C_{L_o}	C_L at C_{D_o}
D	drag
E	aerodynamic efficiency, lift-to-drag ratio, $E = L/D = C_L/C_D$
F_f	rolling or braking friction force
FPA	flightpath angle
F_x	forces along the flightpath axis
F_z	forces perpendicular to the flightpath axis
g	acceleration caused by gravity
k	efficiency factor in quadratic drag equation
L	lift force
L/D	lift-to-drag ratio
$L_{rotation}$	lift force at rotation
q	dynamic pressure
R	range (takeoff or landing distance)
S	area of wing, 3500 ft^2
t	time
T	thrust

TBD	to be determined
V	aircraft speed
V_{CAS}	calibrated airspeed
$V_{touchdown}$	aircraft speed at touchdown
W	aircraft weight
WoW	weight on wheels
x	flightpath axis
z	perpendicular to the flightpath axis
γ	flightpath angle
η	angle between the flightpath angle and the thrust vector
$\theta_{rotation}$	pitch attitude at rotation
μ	coefficient of rolling friction (can include braking effect)

INTRODUCTION

One task an aircraft designer always has in the design of conventional aircraft is determining the inclination of the thrust angle to the fuselage reference line. The optimal inclination is a function of aircraft characteristics and flight phases; and for aircraft with no variable thrust-vectoring capability, the selected inclination angle must be a weighted compromise considering all relevant factors.

The concept behind the optimal thrust inclination angle is simple: if the angle is positive (thrust is tilted down), an additional vertical force is contributed that decreases the lift requirements of the wing. However, this inclination also slightly reduces the horizontal thrust component; thus, an optimization procedure (refs. 1 and 2) is required to determine the optimal angle. This report investigates the relationship of thrust inclination angle for various flight phases. The results can provide insight to the designer for selecting the thrust-vector angle.

Simplified equations of motion are also included for the various flight phases. These sets of equations are then optimized with respect to the thrust inclination angle; the benefits of optimization also are derived from the analysis. The flight regimes investigated are:

- takeoff (minimum takeoff distance).
- climb (maximum rate of climb for a fixed thrust level).
- cruise (minimum thrust; minimum fuel consumption).
- descent (best glide range for a fixed thrust level).
- final approach (minimum approach velocity).
- landing (minimum rollout distance).

The optimization is performed for the full quadratic drag representation, and comparisons are made with a linear drag representation. In addition, an analytical optimization procedure is developed for steady-state flight conditions and the landing rollout. Example results are given for a representative wide-body transport aircraft.

THRUST ANGLE OPTIMIZATION

The ideal inclination of the thrust angle is a function of the particular flight phase. For aircraft with no thrust-vectoring capability, the selected fixed inclination angle depends on the aircraft type and mission; and the selected angle is weighted towards the dominant flight phase. For the few aircraft that currently have—and the future aircraft that will have—thrust-vectoring capability, optimization will change as various flight phases and conditions are encountered.

The equations of motion (ref. 3) are intricate, especially because of the quadratic representation of drag required to assure accurate results. In addition, takeoff and landing conditions are dynamic and thus require time-domain solutions; whereas steady-state flight phases can be analyzed with algebraic solutions. The equations and analysis developed apply equally well to conventional aircraft of all sizes; however, actual results are affected by the aerodynamics of the particular aircraft. Lift and drag characteristics are the most dominant aerodynamics affecting results. The results of the techniques developed herein will be illustrated with a wide-body transport for the different flight phases. The analysis identifies the optimal thrust-vector angle and the accruable benefits. Table 1 shows the flight conditions and required aerodynamics for the flight phases analyzed, which are representative of a typical wide-body transport. Analytical optimization procedures are developed in appendices A and B for steady-state flight conditions and the landing rollout.

OPTIMAL THRUST ANGLE AND BENEFITS FOR TAKEOFF

The optimization objective for the takeoff flight phase is to minimize the distance to aircraft rotation. Figure 1 shows the forces acting on an aircraft at the center of gravity during takeoff acceleration. The resulting equations of motion for takeoff with a thrust-vectoring capability, η, can be written as follows:

$$\sum F_x = 0 = -D + T\cos(\eta) - WA_x/g - F_f; \tag{1}$$

$$\sum F_z = 0 = L + T\sin(\eta) - W + WoW. \tag{2}$$

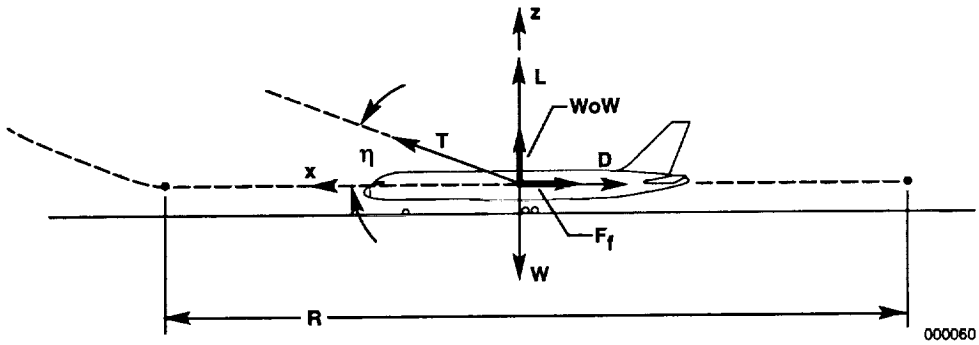

Figure 1. Aircraft forces during takeoff acceleration to rotation.

Table 1. Aircraft parameters and flight conditions.

Variable	Takeoff	Climb	Cruise	Descent	Final approach	Rollout
γ	0	3	0	–3	–3	0
Mach number			0.83	0.80		
V_{CAS}	TBD	300			TBD	
$V_{touchdown}$						120
Altitude	0	15,000	37,000	25,000	4,000	0
W	480,000	460,000	350,000	280,000	280,000	280,000
T	100,000	TBD	TBD	TBD	TBD	–70,000
C_{D_o}	0.050	0.018	0.018	0.018		0.100
k		0.105	0.105	0.105		
C_{L_o}		0.16	0.16	0.16		
C_{L_f}	0.3					
C_L	1.300 at rotation	0.447	0.459	0.228	1.000	0.000
C_D		0.0267	0.0274	0.0185	0.1200	0.100
E		16.80	16.80	12.30	8.33	
μ	0.02					0.40
$\theta_{rotation}$	10.00					

Solving for the weight on wheels, WoW, from equation (2) yields:

$$WoW = W - L - T\sin(\eta). \tag{3}$$

During the horizontal portion of the takeoff acceleration, the lift, L, primarily is caused by flap deflection. The wheel/runway friction force can then be expressed as:

$$F_f = \mu WoW. \tag{4}$$

Rewriting equation (1) using equation (4),

$$A_x = g[T\cos(\eta) - D - \mu WoW]/W, \tag{5}$$

where the drag variation up to the point of rotation is

$$D = qS\left[C_{D_o} + k(C_{L_f} - C_{L_o})^2\right]. \tag{6}$$

The velocity at which the aircraft can take off is the $L_{rotation}$ criterion defined by $L_{rotation} \geq W - T\sin(\eta + \theta_{\text{rotation}})$, where $L_{rotation}$ is the total aircraft lift that would be generated if the aircraft is rotated to the desired pitch attitude, θ_{rotation}, and is a function of velocity defined by

$$L_{rotation} = qS\, C_L, \tag{7}$$

where C_L is a function of angle of attack at the point of rotation.

Equations (5) and (6) cannot be analytically solved for the minimum range, R; time-series solutions must be calculated as follows: Selecting a set of aircraft conditions and a nominal runway friction coefficient, μ; A_x (eq. (5)) is calculated and integrated twice to obtain V and R (eqs. (8) and (9)) for a selected thrust-vector angle, η:

$$A_x = g[T\cos(\eta) - D - \mu WoW]/W \tag{5}$$

$$V = \int A_x\, dt \tag{8}$$

$$R = \int V\, dt \tag{9}$$

Equations (6), (3), and (7) are calculated to obtained updated D, WoW, and $L_{rotation}$ values for the new velocity:

$$D = qS\left[C_{D_o} + k(C_{L_f} - C_{L_o})^2\right] \tag{6}$$

$$WoW = W - L_{rotation} - T\sin(\eta) \tag{3}$$

$$L_{rotation} = qS\, C_L. \tag{7}$$

The $L_{rotation}$ criterion is also calculated at each instant of time: $L_{rotation} \geq W - T\sin(\eta + \theta_{\text{rotation}})$. When the $L_{rotation}$ criterion is met, the aircraft has reached takeoff velocity, thus defining the takeoff distance. (In practice, rotation could start before the $L_{rotation}$ criterion is met because time is needed to rotate the aircraft and during that rotation period, the aircraft has accelerated to a faster speed than required for liftoff.) This analysis is repeated for a range of η.

Figure 2 shows results representative of a wide-body transport for a range of μ; a typical μ for a concrete runway is 0.02. For a given μ, R reduces as the thrust-vector angle increases from 0° to approximately 12°, at which point the minimum takeoff distance is achieved. The thrust-vectoring benefits are modest; R is reduced approximately 200 ft for $\mu = 0.02$. These results are similar for the range of μ presented; however, the benefit of thrust vectoring does increase slightly with increasing μ. The effect of a nominal μ of 0.02 increases takeoff roll approximately 700 ft over the $\mu = 0$ condition; accelerating the aircraft mass with the given level of thrust is the primary factor in determining the takeoff roll distance.

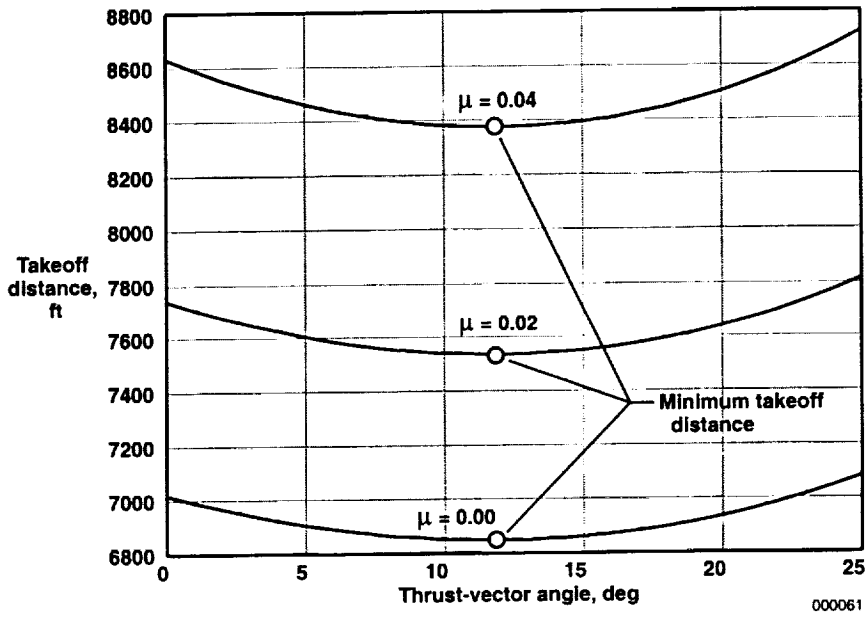

Figure 2. Variation of takeoff distance with thrust-vector angle for various coefficients of rolling friction.

OPTIMAL THRUST ANGLE AND BENEFITS FOR CLIMB, CRUISE, AND DESCENT

The optimization objectives selected for the climb, cruise, and descent flight phases are the maximum rate of climb for a fixed thrust level, minimum thrust (minimum fuel consumption), and the best glide range for a fixed thrust level, respectively.

Because these different flight phases are all steady-state flight, the forces acting on the aircraft can be generalized (fig. 3). The resulting equations of motion for these flight conditions with a thrust-vectoring capability, η, and a flightpath angle (FPA), γ, can be written as follows:

$$\sum F_x = 0 = -D + T\cos(\eta) - W\sin(\gamma); \tag{10}$$

$$\sum F_z = 0 = L + T\sin(\eta) - W\cos(\gamma); \tag{11}$$

where η is measured relative to the flightpath.

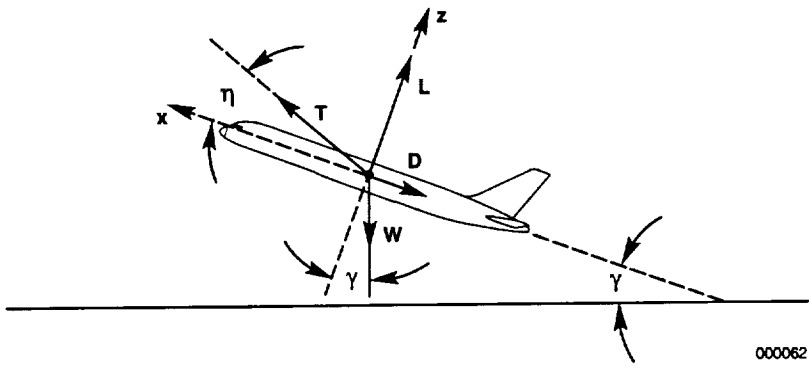

Figure 3. Aircraft forces during steady-state flight phases of climb, cruise, and descent.

Analysis With Quadratic Drag Formulation

Drag can be represented as

$$D = qS\left[C_{D_o} + k(C_L - C_{L_o})^2\right]. \tag{12}$$

Rearranging equation (11) gives

$$L = [W\cos(\gamma) - T\sin(\eta)] = qS\,C_L; \tag{13}$$

substituting C_L from equation (13) into equation (12) gives

$$D = qS\left[C_{D_o} + k\{(W\cos(\gamma) - T\sin(\eta))/(qS) - C_{L_o}\}^2\right]. \tag{14}$$

Rearranging equation (10) gives

$$D = -W\sin(\gamma) + T\cos(\eta). \tag{15}$$

Substituting equation (14) into equation (15),

$$qS\left[C_{D_o} + k\{(W\cos(\gamma) - T\sin(\eta))/(qS) - C_{L_o}\}^2\right] = T\cos(\eta) - W\sin(\gamma). \tag{16}$$

Expanding equation (16) and collecting thrust, T, terms in the form

$$aT^2 + bT + c = 0 \tag{17}$$

produces the coefficients

$$a = \sin(\eta)^2;$$

$$b = -2W\cos(\gamma)\sin(\eta) + 2qS\,C_{L_o}\sin(\eta) - qS\cos(\eta)/k; \text{ and}$$

$$c = W^2\cos(\gamma)^2 - 2qSWC_{L_o}\cos(\gamma) + q^2S^2C_{L_o}{}^2 + q^2S^2C_{D_o}/k + qSW\sin(\gamma)/k.$$

Selecting a set of aircraft conditions including FPA, the quadratic equation (17) is solved for thrust, T, for specific thrust-vector angles, η. Only one solution of the quadratic equation provides meaningful results. (For the examples calculated, the thrust produced by the other root is of the order of 10^{14} at $\eta = 0$.) Plotting thrust as a function of thrust-vector angle will provide the optimal thrust-vector angle for minimum thrust required for steady-state flight at the selected FPA. These results apply to climb, cruise, and descent flight conditions, depending on the FPA selected.

Climb Conditions

Figure 4 shows results for a nominal climb FPA of 3°. For this nominal FPA, a minimum thrust condition is achieved at a thrust-vectoring angle of approximately 3.4° and results in a thrust reduction of approximately 90 lbf. Also plotted are data for a FPA of 3.0115° (fig. 4). A comparison of the two sets of data shows that for a constant thrust setting, optimal thrust vectoring increases the FPA 0.0115°, a 0.38-percent increase.

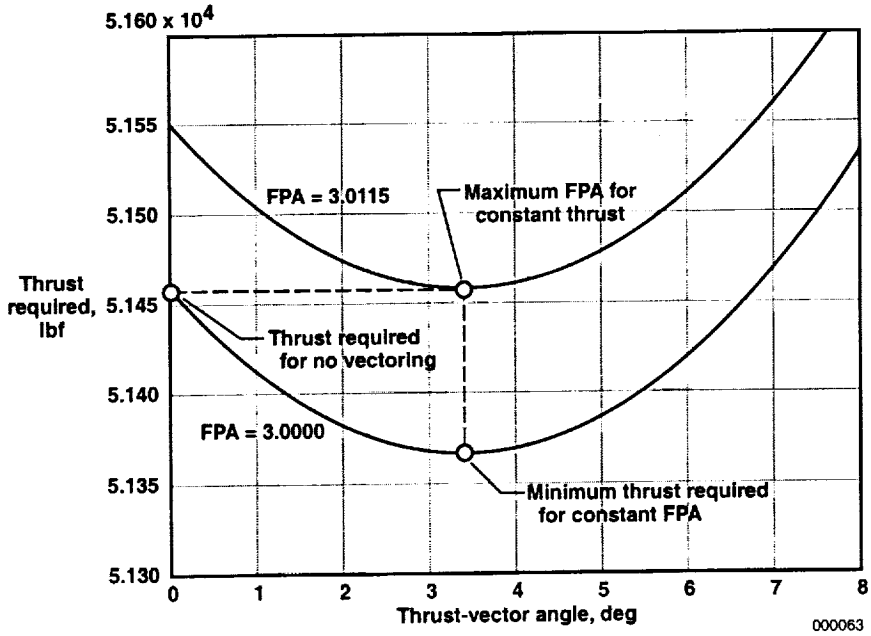

Figure 4. Variation of thrust required with thrust-vector and flightpath angles in a climb.

Cruise Conditions

Figure 5 shows results for a level cruise flight condition. For this cruise condition, a minimum thrust condition is achieved at a thrust-vectoring angle of approximately 3.6° and results in a thrust reduction of approximately 40 lbf.

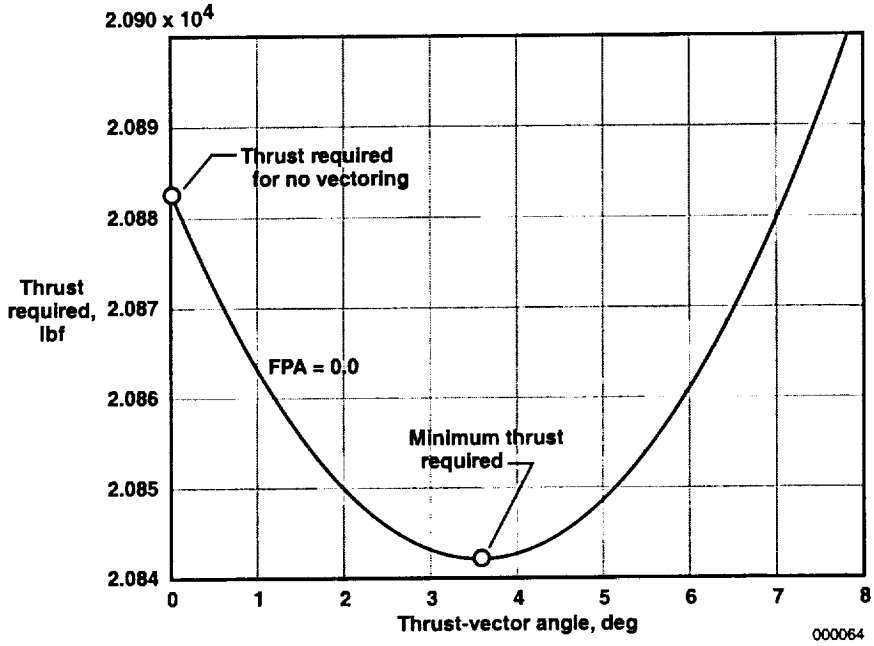

Figure 5. Variation of thrust required with thrust-vector angle for cruise flight.

Although the benefit is small for the cruise flight phase, the takeoff-to-landing benefit is greater, percentage-wise, than the instantaneous benefit at any one flight condition. This greater benefit is caused by the cumulative effects of reduced fuel consumption for the entire cruise portion of flight and also includes the fact that not as much fuel has to be loaded for takeoff. This same cumulative benefit applies to the climb flight phase, although the benefit is smaller because of the short amount of time required to climb to cruise conditions. The beginning-to-end calculation of benefits is beyond the scope of this report; however, a representative penalty incurred carrying unnecessary fuel is approximately 4 lbm/hr for each 100 lbm of fuel carried.

Descent Conditions

Figure 6 shows results for a nominal descent FPA of –3°. For this nominal FPA, a minimum thrust condition is achieved at a thrust-vectoring angle of approximately 0.8° and results in a thrust reduction of less than 1 lbf. Optimization is minimal at this flight condition because of the fact that the thrust level required for this descent flight condition is low. As the thrust level approaches 0 lbf, the benefit of the vectoring thrust approaches 0 percent. The best glide range for any aircraft with 0-lbf thrust is proportional to the lift-to-drag ratio, L/D, and is defined by the relation $\gamma \approx -1/(L/D)$.

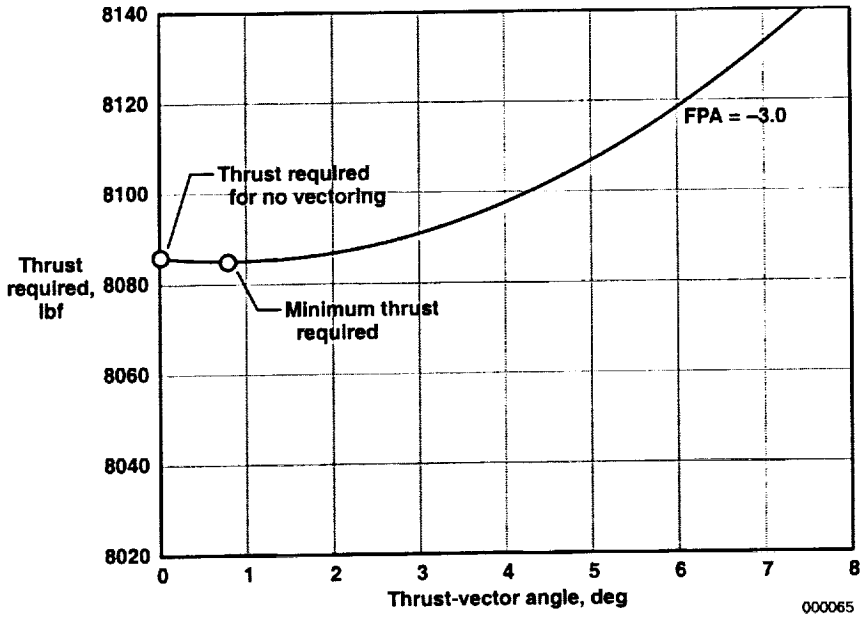

Figure 6. Variation of thrust required with thrust-vector angle in a descent.

Analysis With Simplified Drag Formulation

In situations where the aircraft is operating near its best aerodynamic efficiency, the L/D can be used for obtaining qualitative results. Representing L/D by E, an expression for drag is $D = L/E$. Substituting this expression into equation (10) and solving simultaneously with equation (11) will produce thrust as a function of the aircraft weight; FPA; thrust-vector angle; and E:

$$T = W[\sin(\gamma) + E^{-1}\cos(\gamma)]/[\cos(\eta) + E^{-1}\sin(\eta)]. \tag{18}$$

Figures 7–9 show the results of this simplified formulation compared with the previous results for the climb, cruise, and descent results (figs. 4–6).

For the climb condition (fig. 7), the complete and simplified results are essentially identical. For the cruise condition (fig. 8), the simplified result provides a very good approximation and indicates only a slight reduction in both the optimal thrust-vector angle and the thrust required. For the descent condition (fig. 9), the results are significantly different: although the complete analysis indicated essentially no benefit for thrust vectoring, the simplified analysis indicates a thrust reduction benefit of 23 lbf at a thrust-vectoring angle of approximately 4.7°. The difference for the descent flight condition is mainly caused by the fact that the linear representation of drag as a function of lift is significantly different than the quadratic drag representation. The linear representation of drag agrees with the quadratic representation of drag only near the maximum L/D for the aircraft, which is generally where aircraft are designed to cruise (thus the good agreement for the cruise flight condition).

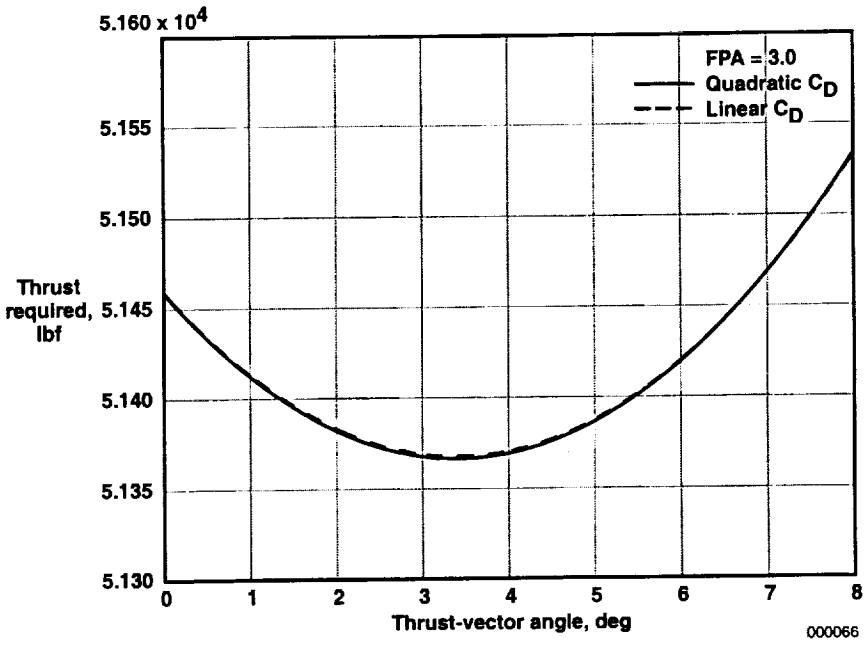

Figure 7. Comparison of climb thrust required with thrust-vector angle for a quadratic and linear drag representation.

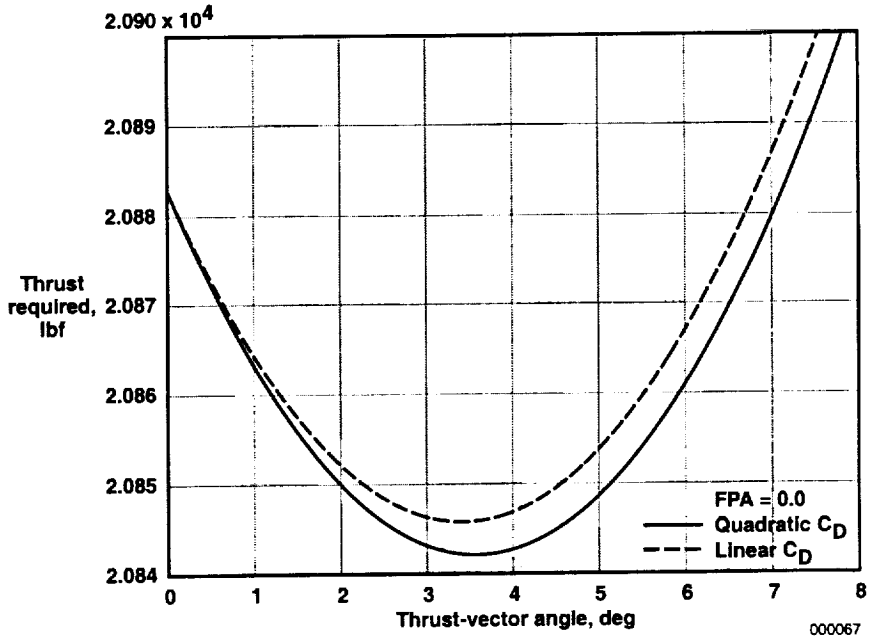

Figure 8. Comparison of cruise thrust required with thrust-vector angle for a quadratic and linear drag representation.

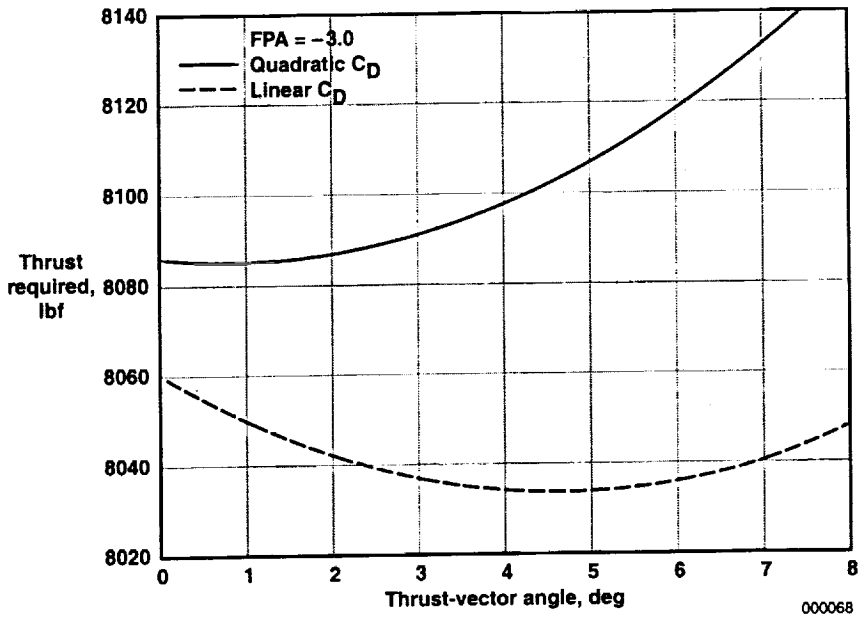

Figure 9. Comparison of descent thrust required with thrust-vector angle for a quadratic and linear drag representation.

Analytical Optimization

For the simplified formulation, the optimal thrust-vector angle can be analytically determined for the climb, cruise, and descent flight phases. Appendix A shows the development of the optimal angle. The resulting optimization relationship for thrust-vector angle is $\tan(\eta) = 1/E$.

Interestingly, the parameter E totally defines the optimization result. These analytical results are identical to the optimal thrust-vectoring angle obtained from the simplified analysis (table 2). The results from the complete analysis are similar for the climb and cruise flight phases, but are significantly different for the descent phase.

Table 2. Comparison of optimal thrust-vector angle, η, for the various analysis techniques.

	Flight phase		
η	Climb, deg	Cruise, deg	Descent, deg
Complete analysis	3.4	3.6	0.8
Simplified analysis	3.4	3.4	4.6
Analytical expression	3.4	3.4	4.6

OPTIMAL THRUST ANGLE AND BENEFITS FOR FINAL APPROACH

The optimization objective selected for the final approach flight phase is to minimize approach velocity, which will result in a reduced rollout distance when touchdown occurs. The steady-state equations of motion for the final approach are the same as those in the previous section for climb, cruise, and descent. The difference is that in the previous examples, maximizing aerodynamic efficiency was the objective; whereas in the final approach, a minimum touchdown speed is the objective. This minimized touchdown speed will be obtained at a higher thrust level than would be required for an approach condition with no thrust vectoring.

Repeating equations (10) and (11), $\sum F_x = 0 = -D + T\cos(\eta) - W\sin(\gamma)$; $\sum F_z = 0 = L + T\sin(\eta) - W\cos(\gamma)$. Solving each equation for η,

$$\cos(\eta) = [D + W\sin(\gamma)]/T; \tag{19}$$

$$\sin(\eta) = [W\cos(\gamma) - L]/T. \tag{20}$$

Dividing equation (20) by equation (19) yields:

$$\tan(\eta) = [W\cos(\gamma) - L]/[D + W\sin(\gamma)]. \tag{21}$$

The intersections of any two of the three equations (19)–(21) for various γ and thrust levels will provide trimmed flight conditions. However, because equation (21) is not a function of thrust, it provides a single curve, a locus of trimmed solutions as a function of γ. Equations (21) and (19) are then used to obtain thrust-vector angle optimization.

Figure 10 shows aircraft velocity as a function of thrust-vector angle and thrust level for $\gamma = -3.0°$; trimmed flight conditions are indicated by the dashed line. In general, increased thrust levels clearly will permit significant decreases in aircraft velocity. For the descent conditions with no thrust-vectoring angle, the velocity is approximately 279 ft/sec at a thrust level of approximately 18,900 lbf. However, if the aircraft were trimmed at a thrust level of 60,000 lbf and a vectoring angle of approximately 78°, the aircraft could be flown at a stabilized velocity of approximately 248 ft/sec; more than 30 ft/sec slower than without vectoring and a more than 10-percent reduction in approach speed.

Figure 11 shows that at low vectoring angles, the aircraft can be trimmed at the same thrust (18,900 lbf) but with a vector angle of 13.5°, thus reducing approach speed by a little more than 2 ft/sec. At a vector angle of approximately 7°, the thrust can be reduced approximately 130 lbf and still maintain the same FPA.

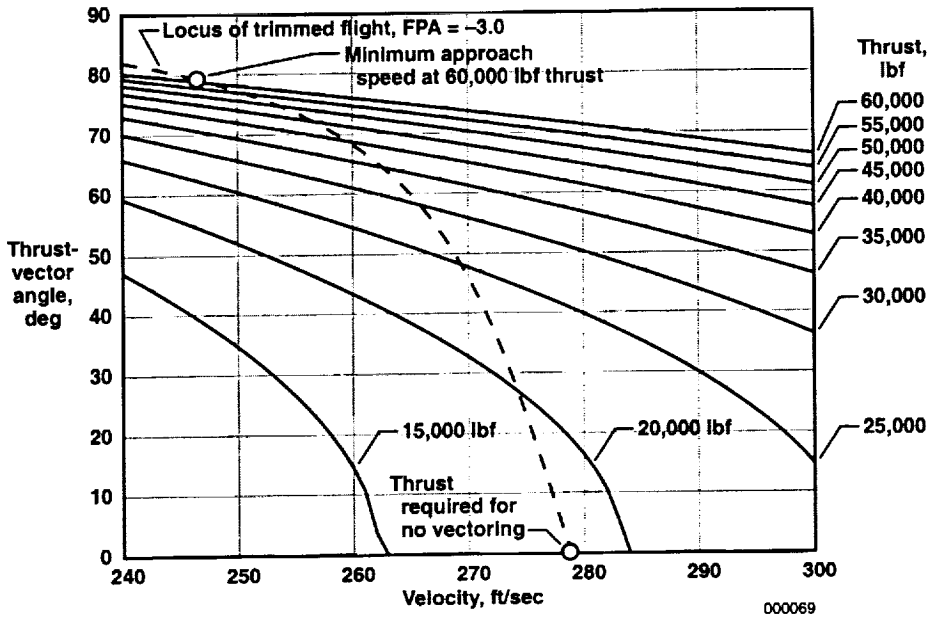

Figure 10. Variation of approach speed with thrust-vector angle and thrust.

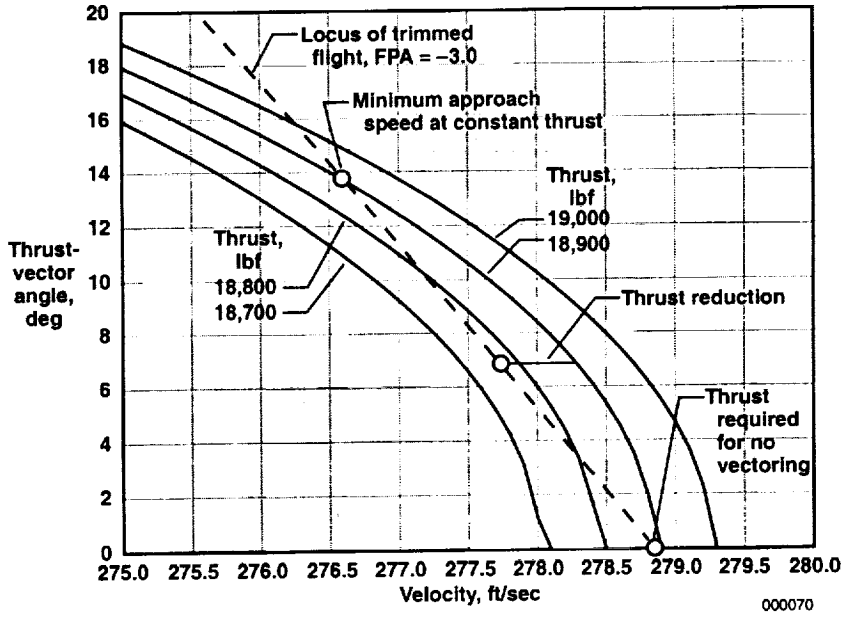

Figure 11. Variation of approach speed with thrust-vector angle and thrust.

OPTIMAL THRUST ANGLE AND BENEFITS FOR LANDING ROLLOUT

The optimization objective selected for the landing rollout flight phase is to minimize rollout distance when the aircraft has touched down. Figure 12 shows the forces acting on an aircraft during the landing rollout. The steady-state equations of motion for the landing with a thrust-vectoring capability, η, can be written as follows:

$$\sum F_x = 0 = -D + T\cos(\eta) - WA_x/g - F_f; \tag{22}$$

$$\sum F_z = 0 = L + T\sin(\eta) - W + WoW. \tag{23}$$

These equations are identical to the takeoff roll equations (eqs. (1)–(2)). Assuming that the lift, L, is 0 lbf because of spoiler and speedbrake deflection, solving for the weight on wheels, WoW, from equation (23) is expressed as

$$WoW = W - T\sin(\eta). \tag{24}$$

The drag variation during the rollout can be expressed as

$$D = qS\,C_{D_o}. \tag{25}$$

Positive thrust is defined as positive in the forward direction; therefore, for the landing rollout condition where thrust will be reversed, thrust (T) will have a negative value. This definition implies that when the thrust is reversed, a positive η will provide a downward thrust component, thus increasing the rolling friction force as

$$F_f = \mu(WoW). \tag{26}$$

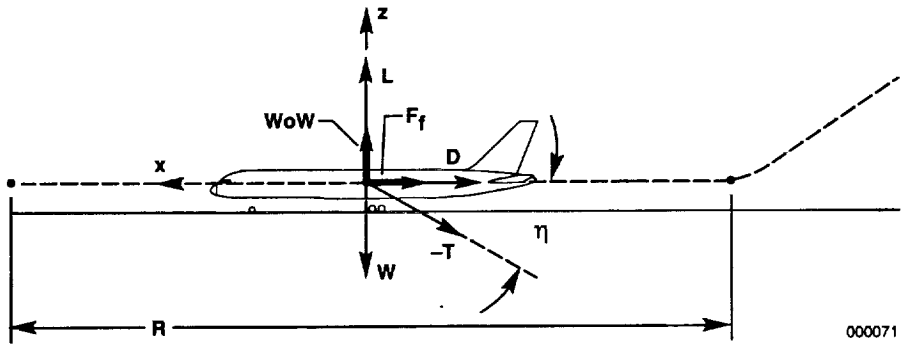

Figure 12. Aircraft forces from touchdown and through deceleration to a stopped condition.

Rewriting equation (22) and solving using a time-series method is calculated as follows: Selecting a set of aircraft conditions and a runway surface coefficient, μ; equations (27), (28), (29), (25), and (24) are calculated for a selected thrust-vector angle, η:

$$A_x = g[T\cos(\eta) - D - \mu WoW]/W; \tag{27}$$

$$V = V_{touchdown} + \int A_x \, dt; \tag{28}$$

$$R = \int V dt; \tag{29}$$

$$D = qS\, C_{D_o}; \text{ and} \tag{25}$$

$$WoW = W - T\sin(\eta). \tag{24}$$

The landing rollout starts with a touchdown velocity equivalent to a calibrated airspeed of 120 kn. The time at which the forward velocity equals 0 kn defines when the aircraft has stopped. This analysis can repeated for a range of η.

Figure 13 shows rollout distance results as a function of thrust-vector angle and μ for a wide-body transport at touchdown conditions. The thrust is –70,000 lbf (reversed); $C_{D_o} = 0.10$; and the nominal $\mu = 0.4$ (which includes the effect of near maximum braking capability). For this configuration, the optimal thrust-vector angle is approximately 22° and has reduced the rollout distance approximately 26 ft (2.7 percent). Also shown is the effect of μ, which is the most important factor in decelerating the aircraft.

Figure 14 shows rollout distance as a function of time to stop for the same data as figure 13 with $\mu = 0.4$, and shows that the time to stop is reduced by approximately 0.26 sec (2.8 percent). In addition to the benefits of optimization being small, the rollout distance and time to stop are quite short. This shortness is because of the model used, which assumes the application of the friction caused by braking, the drag effect caused by spoilers, and reverse thrust all are applied at the instant of touchdown. Commercial aircraft typically have many seconds after touchdown before these various items are activated. In any case, the incremental changes indicated by this analysis are representative of actual results. Figure 15 shows the effect of C_{D_o} and thrust. The C_{D_o} has a minor effect on rollout distance; thrust has a significant effect on rollout distance.

Appendix B develops the following simplified optimization expression for η, which produces the minimum landing rollout distance: $\tan(\eta) = \mu$. These results are identical to the optimal thrust-vectoring angle obtained from the complete analysis (table 3).

Table 3. Comparison of optimal thrust-vector angle, η, for various analysis techniques.

	μ		
η	0.30	0.40	0.50
Complete analysis	17°	22°	27°
Analytical expression	17°	22°	27°

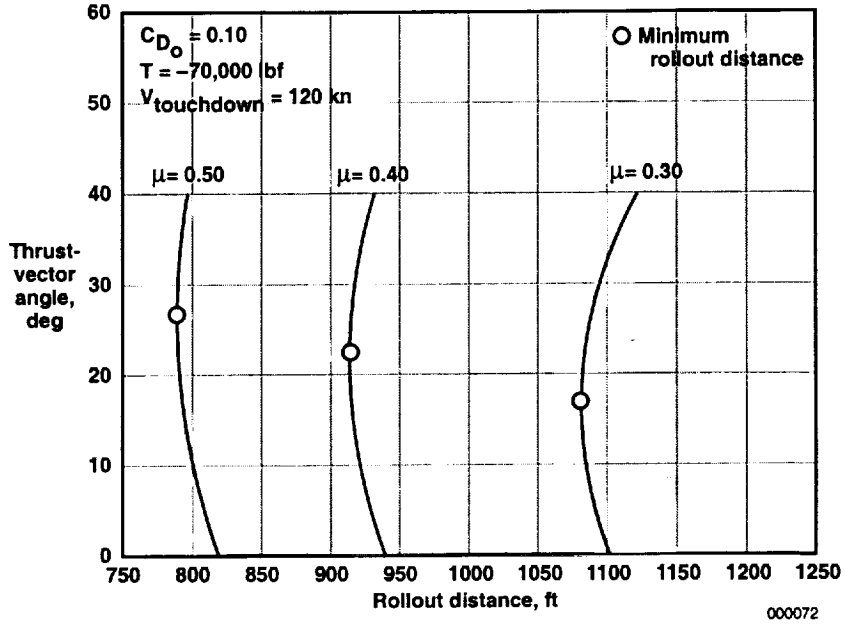

Figure 13. Variation of rollout distance with thrust-vector angle and coefficient of braking friction.

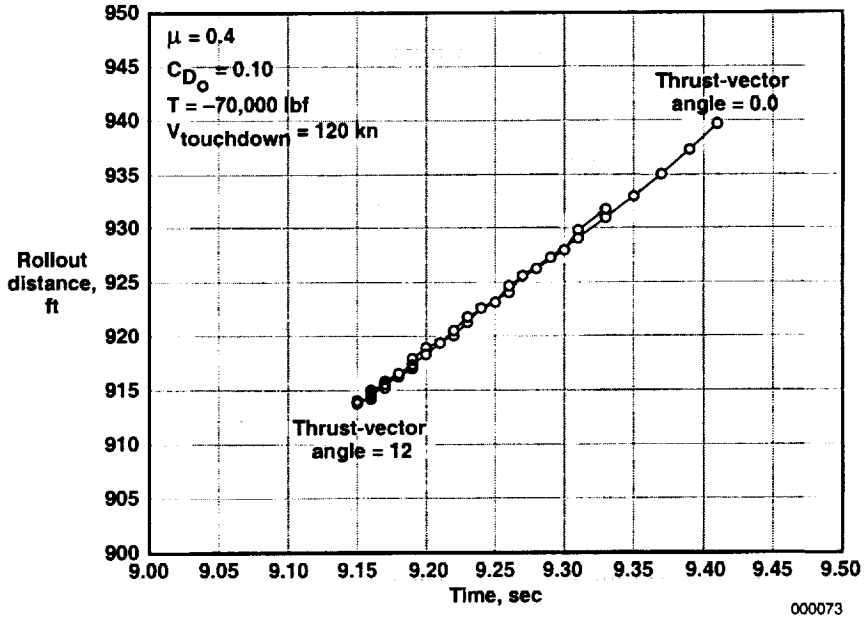

Figure 14. Variation of rollout distance and time to stop with thrust-vector angle.

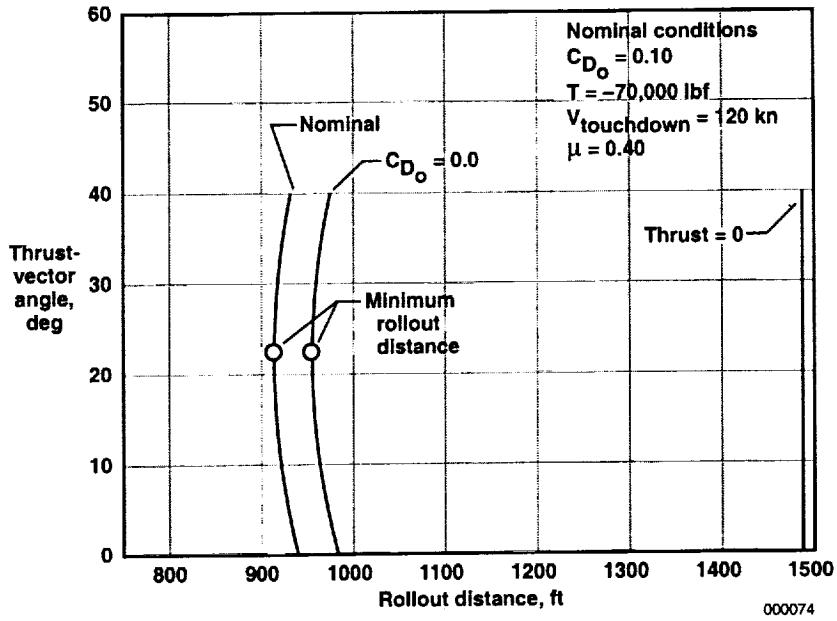

Figure 15. Variation of rollout distance with thrust-vector angle, C_{D_o}, and thrust, T.

CONCLUDING REMARKS

Analyses were performed to determine optimal thrust-vector angle as a function of various flight conditions. The flight regimes explored were takeoff, climb, cruise, descent, final approach, and landing. The equations developed for the various flight phases are simplifications of actual conditions, but the resulting relationships accurately depict the optimal thrust-vector trends and provide an indication to the aircraft or propulsion controls designer. Results for a typical wide-body transport are as follows:

Phase	Optimization	Improvement, percent	η, deg
Takeoff	Distance	Reduced 2.5	12.0
Climb	Rate of climb	Increased 0.4	3.4
Cruise	Thrust	Reduced 0.2	3.6
Descent	Glide range	No improvement	0.8
Final approach	Velocity	Reduced ≈10.0	≈ 78.0
Landing rollout	Distance	Reduced 2.8	22.0

Analytical optimization developed two expressions for the optimal thrust-vector angle: one as a function of runway friction coefficient for the landing condition, and the other as a function of the lift-to-drag ratio, L/D, for all the "up-and-away" flying conditions. These results compared very well for

the climb, cruise, and landing rollout flight phases. The process easily can be extended to complex aircraft configurations and flight conditions.

Generalized observations for the various flight phases are as follows:

- **Takeoff:** Thrust-to-weight ratio dominates, and increasing values give faster acceleration and increased optimal thrust-vectoring angles and associated benefits.
- **Climb, cruise, and descent:** Lower L/D configurations benefit most from thrust vectoring because of larger optimal thrust-vector angles.
- **Final approach:** High thrust-to-weight configurations benefit most, assuming very large thrust-vectoring angles can be achieved.
- **Rollout:** The runway friction coefficient is dominant, although large levels of reversed thrust would be beneficial.

Dryden Flight Research Center
National Aeronautics and Space Administration
Edwards, California, March 7, 2000

APPENDIX A

OPTIMAL THRUST ANGLE FOR STEADY-STATE FLIGHT

The steady-state equations of motion for climb, cruise, and descent flight phases with a thrust-vectoring capability, η, and a flightpath angle, γ, can be written as follows:

$$\sum F_x = 0 = -D + T\cos(\eta) - W\sin(\gamma); \tag{A-1}$$

$$\sum F_z = 0 = L + T\sin(\eta) - W\cos(\gamma). \tag{A-2}$$

Rewriting equation A-2,

$$L = W\cos(\gamma) - T\sin(\eta). \tag{A-3}$$

Defining $E = L/D$; thus,

$$D = L/E. \tag{A-4}$$

Substituting expression (A-4) into equation (A-1) and then substituting equation (A-3) into equation (A-1) results in

$$0 = -WE^{-1}\cos(\gamma) + TE^{-1}\sin(\eta) + T\cos(\eta) - W\sin(\gamma).$$

Solving for T,

$$T = W[\sin(\gamma) + E^{-1}\cos(\gamma)]/[\cos(\eta) + E^{-1}\sin(\eta)]. \tag{A-5}$$

To find the minimum thrust, T, with respect to η, the necessary condition is that the partial derivative $\partial T/\partial\eta = 0$; thus:

$$\begin{aligned}\partial T/\partial\eta &= 0 \\ &= [\{\cos(\eta) + E^{-1}\sin(\eta)\}\{0\} - W\{\sin(\gamma) + E^{-1}\cos(\gamma)\}\{-\sin(\eta) + E^{-1}\cos(\eta)\}] \\ &\quad /[\cos(\eta) + E^{-1}\sin(\eta)]^2.\end{aligned} \tag{A-6}$$

Upon reducing and assuming $\{\sin(\gamma) + E^{-1}\cos(\gamma)\} \neq 0$,

$$0 = -\sin(\eta) + E^{-1}\cos(\eta).$$

Rearranging:

$$\tan(\eta) = 1/E.$$

The above analysis assumes the sign of η is positive, which is intuitive for cruise flight. The singularity point where $\{\sin(\gamma) + E^{-1}\cos(\gamma)\} = 0$ defines the best glide angle ($\tan(\gamma) = -1/(L/D)$) for $T = 0$, which in turn is derived from equation (A-5).

APPENDIX B

OPTIMAL THRUST ANGLE FOR LANDING ROLLOUT

The key parameter to be optimized in the landing rollout condition is the distance required to decelerate from touchdown to a stopped aircraft. This parameter can be expressed as:

$$R = \int V dt, \tag{B-1}$$

where the velocity, V, is expressed as

$$V = V_{touchdown} + \int A_x \, dt \tag{B-2}$$

and the deceleration, A_x, developed in the "Optimal Thrust Angle and Benefits for Landing Rollout" section and expressed in equation (25), is:

$$A_x = g[T\cos(\eta) - D - \mu(W - T\sin(\eta))]/W. \tag{B-3}$$

To find the maximum of A_x with respect to η, the necessary condition is that the partial derivative $\partial A_x/\partial\eta = 0$, because maximizing the deceleration will minimize the landing rollout distance, R. Thus, $\partial A_x/\partial\eta = 0 = [g[(T) - \sin(\eta) - (0) - (0) + (\mu T)(\cos(\eta))]]/W$. Upon reducing, $0 = -\sin(\eta) + \mu\cos(\eta)$. Rearranging, $\tan(\eta) = \mu$.

The sign of η is positive, which provides an additional down force on the wheels when thrust is reversed, thus increasing the rolling friction. The final result is the same for takeoff if the rotation velocity is assumed constant; however, as shown in this report, the vertical component of thrust reduces lift required for takeoff and thus the rotation velocity.

REFERENCES

1. Bolonkin, A. A., *New Methods of Optimization and their Applications*, Moscow Highest Technical University named Bauman, Moscow, 1972.

2. Bolonkin, Alexander and Narenda Khot, "Method for Finding a Global Minimum," AIAA-94-4420, Jan. 1994.

3. McCormick, Barnes W., *Aerodynamics, Aeronautics, and Flight Mechanics*, John Wiley & Sons, New York, 1979.

REPORT DOCUMENTATION PAGE

Form Approved
OMB No. 0704-0188

1. AGENCY USE ONLY (Leave blank)	2. REPORT DATE	3. REPORT TYPE AND DATES COVERED
	March 2000	Technical Memorandum

4. TITLE AND SUBTITLE

Optimal Pitch Thrust-Vector Angle and Benefits for all Flight Regimes

5. FUNDING NUMBERS

WU 522-16-14-00-39-00-LIO

6. AUTHOR(S)

Glenn B. Gilyard and Alexander Bolonkin

7. PERFORMING ORGANIZATION NAME(S) AND ADDRESS(ES)

NASA Dryden Flight Research Center
P.O. Box 273
Edwards, California 93523-0273

8. PERFORMING ORGANIZATION REPORT NUMBER

H-2402

9. SPONSORING/MONITORING AGENCY NAME(S) AND ADDRESS(ES)

National Aeronautics and Space Administration
Washington, DC 20546-0001

10. SPONSORING/MONITORING AGENCY REPORT NUMBER

NASA/TM-2000-209021

11. SUPPLEMENTARY NOTES

Glenn B. Gilyard, NASA Dryden Flight Research Center, Edwards, California and Alexander Bolonkin, Senior Research Associate of the National Research Council, Edwards, California.

12a. DISTRIBUTION/AVAILABILITY STATEMENT

Unclassified—Unlimited
Subject Category 02-01, 02-03, 03-01

This report is available at http://www.dfrc.nasa.gov/DTRS/

12b. DISTRIBUTION CODE

13. ABSTRACT (Maximum 200 words)

The NASA Dryden Flight Research Center is exploring the optimum thrust-vector angle on aircraft. Simple aerodynamic performance models for various phases of aircraft flight are developed and optimization equations and algorithms are presented in this report. Results of optimal angles of thrust vectors and associated benefits for various flight regimes of aircraft (takeoff, climb, cruise, descent, final approach, and landing) are given. Results for a typical wide-body transport aircraft are also given. The benefits accruable for this class of aircraft are small, but the technique can be applied to other conventionally configured aircraft. The lower L/D aerodynamic characteristics of fighters generally would produce larger benefits than those produced for transport aircraft.

14. SUBJECT TERMS	15. NUMBER OF PAGES
Commercial aircraft, Efficiency, Lift-to-drag ratio, Optimization, Thrust vectoring	28
	16. PRICE CODE: A03

17. SECURITY CLASSIFICATION OF REPORT	18. SECURITY CLASSIFICATION OF THIS PAGE	19. SECURITY CLASSIFICATION OF ABSTRACT	20. LIMITATION OF ABSTRACT
Unclassified	Unclassified	Unclassified	Unlimited

NSN 7540-01-280-5500

Standard Form 298 (Rev. 2-89)
Prescribed by ANSI Std. Z39-18
298-102